

# Large-area picosecond laser-induced periodic surface structure (LIPSS) on chromium

L. Bayer<sup>a,\*</sup>, M. Ehrhardt<sup>a</sup>, P. Lorenz<sup>a</sup>, M. Mäser<sup>b</sup>, K. Zimmer<sup>a</sup>

<sup>a</sup>Leibniz-Institut für Oberflächenmodifizierung e. V., Permoserstraße 15, 04318 Leipzig, Germany

<sup>b</sup>SWG, Badstraße 9, 09669 Frankenberg, Germany

---

## Abstract

In the field of packaging in particular advertising and product security new applications, technologies and production technics are demanded. This paper shows the formation of laser-induced periodic surface structures (LIPSS) on flat and cylindrical surfaces using an ultrashort pulsed laser. These structures have due to their micro-sized strong periodic characteristics a remarkable spectral optical effect. The used laser provides a beam with a wavelength of 1064 nm and a pulse length of 13 ps. In the experimental series the fluence as well as the number of pulses were changed to find the most optimal parameter field. Furthermore, a fast large-area production test of LIPSS on Cr-coated Cu embossing sleeves was performed. Therefor a fast scanning polygon scanner was used to achieve a high-resolution multi-directional LIPSS in a reasonable commercial attractive time.

© 2016 The Authors. Published by Bayerisches Laserzentrum GmbH

*Keywords:* LIPSS; cylindrical surfaces; picosecond; spectral optical effect

---

## 1. Introduction

The packaging industry is constantly searching for new innovative possibilities for advertising or product security applications. In this paper a method is investigated to generate laser-induced periodic surface structures (LIPSS) on flat and cylindrical metal surfaces. Especially in this area of applications two effects of LIPSS could be interesting. Due to the strong periodic wave structure a spectral optical effect can be achieved. Using a white light source, light with a specific wavelength can be observed under a certain viewing angle (rainbow effect) [1]. The second effect is that LIPSS can create (super)hydrophobic surfaces under certain circumstances or with additional treatment [2, 3]. Both effects are very attractive for packaging applications. Structured cylinders or sleeves could be used as an embossing form. In this case the LIPSS could be copied on polymer foils via heat embossing techniques transferring also their optical and surface characteristics.

The formation of laser-induced periodic surface structures (LIPSS) was investigated many times, especially for laser pulses with a pulse duration in the range of femtoseconds [1, 2, 4-10]. However, the use of picosecond [3, 11, 12] or nanosecond pulses [13] for LIPSS structuring is less frequently presented in the literature. LIPSS can be created on metals as well as on semiconductors or polymers [4, 5, 14]. In general, two main types of LIPSS are discussed: low spatial frequency LIPSS (LSFL) and high spatial frequency LIPSS (HSFL). In this paper only the LSFL LIPSS are considered and discussed.

The formation of LSFL LIPSS can be explained by the interference between the incident laser light and the scattered light [6, 15] or a surface plasmon polarization [10]. However, the spatial period of this wave structure  $\Lambda$  is dependent on the used laser wavelength  $\lambda$  and the angle of incidence  $\theta$ . This can be described with the following equation (1) [6]:

$$\Lambda = \frac{\lambda}{1 \pm \sin \theta} \quad (1)$$

---

\* Corresponding author. Tel.: +49-341-235-3287; fax: +49-341-235-2584 .  
E-mail address: Lukas.bayer@iom-leipzig.de

For all experiments in this paper the angle of incidence was fixed at  $0^\circ$ . Considering this, the spatial period of the wave structure is equal to the wavelength of the laser light. This could be confirmed by all the done experiments for this paper. The orientation of the wave structure is also connected with a laser beam parameter, in this case: the polarization of the laser beam [9]. If the beam is linearly polarized the orientation of the LIPSS can be rotated by rotating the polarization. This can be done with a half-wave plate.

## 2. Experimental set-up

The overall experimental set-up is shown in Fig. 1. It consists of three main parts: a laser, a scanning and a sleeve holding system. All parts were installed in a 3D Micromac microSTRUCT vario workstation (not by default). The used EKSPLA Atlantic picosecond DPSS laser provides a Gaussian laser beam ( $\sim 60 \mu\text{m}$  focused diameter) with a wavelength of 1064 nm and a pulse length of 13 ps. The pulse frequency can be set up to 1 MHz using a power of up to 60 W. The laser fluence can be changed by adjusting an attenuator. The scanning of the beam was performed by a Next Scan Technology LSE170 polygon scanner. Unlike common mirror scanning systems this scanner uses a constantly rotating octagonal polygon mirror unit to scan the laser beam with a speed between 25 and 100 m/s. The scanner provides a scan width of 170 mm. Due to the scanning technique the beam can be only scanned in one direction. To generate a large-area surface structure a secondary axis was needed. Therefore, two systems were used: For small planar samples a normal linear axis and for the large metal sleeves a rotational axis with matching pneumatic sleeve system. In addition to this more linear tables are used to regulate the position of focus and to place the roll precisely under the scanning system. The entire beam path has a length of 5 m. This has no effect on the quality of the beam. To set a defined polarization of the beam a half-wave plate was used.

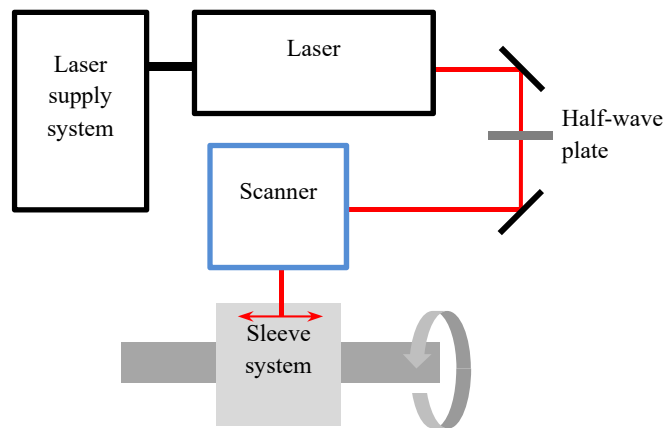


Fig. 1. Schematic sketch of the experimental set-up.

All experiments are performed on the same type of metal sleeves. Sleeve systems are commonly used in the printing and packaging industry to avoid heavy solid printing or embossing cylinders. Metal sleeves are wide metal rings in which the transfer pattern is engraved. The sleeves used for the experiments are 14 cm wide and have a radius of 11 cm. For small tests one of the sleeves was cut in smaller pieces  $\sim 2 \text{ cm} \times 3 \text{ cm}$ . All samples have three layers as shown in Fig. 2. The lowest layer consists of  $100 \mu\text{m}$  nickel. Upon this a  $350 \mu\text{m}$  thick copper layer and a chromium layer ( $10 \mu\text{m}$ ) is deposited. All metal layers are created by electro-plating.

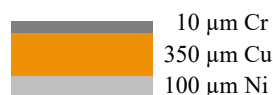


Fig. 2. Layer system of sample sleeves.

## 3. Experimental results

### 3.1. General formation of LIPSS

To find an optimal parameter set for the LIPSS formation a test array was produced by scanning lines with varying the scanning speed (number of pulses) and the laser power. The result can be seen in Table 1. The field of parameter sets where continuously LIPSS are formed is surrounded by three main problematics: With lower laser power the spot diameter decreases. This leads to a separation of the spots and a discontinuous line. With high

laser power and a small number of pulses only a melting of the surface is observed. Lines produced with a high laser power and a large number of laser pulses show droplet formations instead of LIPSS. Two examples can be seen in Fig. 3. The left image shows continuous LIPSS, the right image droplet formation.

Table 1. Results of line arrays by varying number of pulses and laser power.

		Laser fluence [ $J/cm^2$ ]												
		1.08	0.98	0.87	0.76	0.65	0.54	0.44	0.33	0.22	0.11	0.09	0.07	0.04
Number of Pulses	10													
	20													
	30													
	40													
	50													
	60													
	70													
	80													
	90													
	100													

	no modification
	modification but no LIPSS
	pulses separate – LIPSS are continuously
	to small overlap - LIPSS not continuously
	LIPSS with melting in beam centre
	LIPSS continuously
	LIPSS with droplet formation

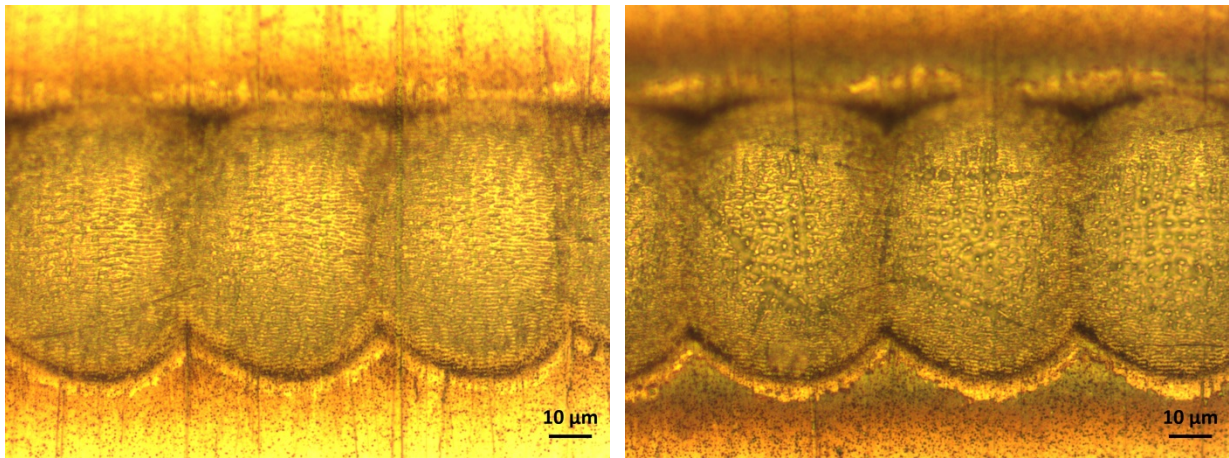


Fig. 3. Optical microscopic images of lines with a laser power of 30 W, pulse spacing 50  $\mu m$ , 20 pulses (left), 80 pulses (right). Pulses are perfectly scanned over each other.

### 3.2. Orientation of LIPSS

The orientation of the wave structure can be controlled by changing the laser polarization. For this experiment a half-wave plate was used to set a specific linear laser polarization angle.

Fig. 4 shows how the wave orientation is rotated by rotating the half-wave plate.

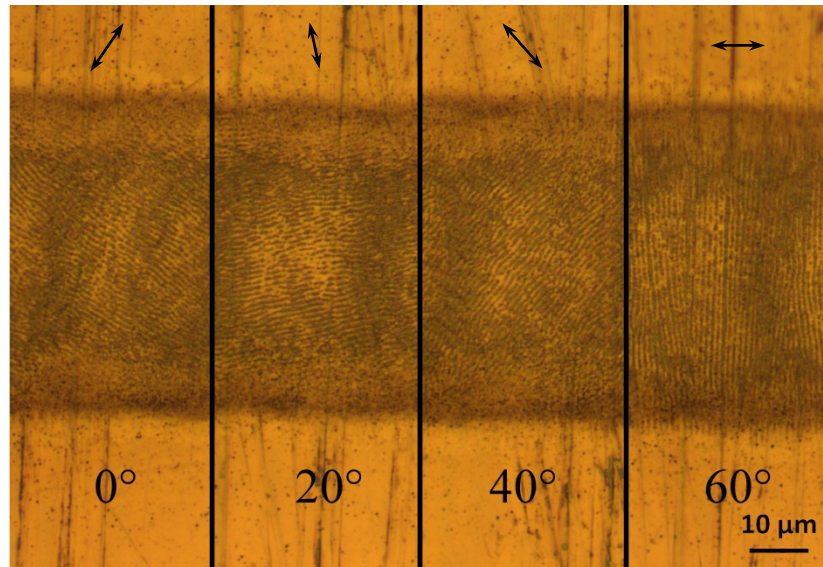


Fig. 4. Optical microscopic images of different wave orientations at different rotation angles of the half-wave plate (numbers show plate angle; double arrows indicate the direction of the electrical field of the laser beam).

#### 4. Fast process of large-area LIPSS

To cover an area with LIPSS lines with a defined pulse spacing  $s_p$  are scanned under each other with a constant line spacing  $s_l$ . If these two parameters are set to the value of the spot diameter ( $\sim 65 \mu\text{m}$  at  $0.6 \text{ J/cm}^2$ ) the dots exactly match together. To achieve a completely covered surface these values must be smaller. It is clear that these two values directly control the number of laser pulses per position. To reach the necessary 20–50 pulses these parameters must be small. The smallest possible spacing of the pulses in each line is limited by the scanner with  $28 \mu\text{m}$  (overlap  $\sim 57\%$ , 2 pulses per position in line). So the line spacing must be much smaller. To reach an acceptable number of pulses and a uniform surface a line space of  $3 \mu\text{m}$  (overlap  $\sim 95\%$ , 22 pulses per position) was used.

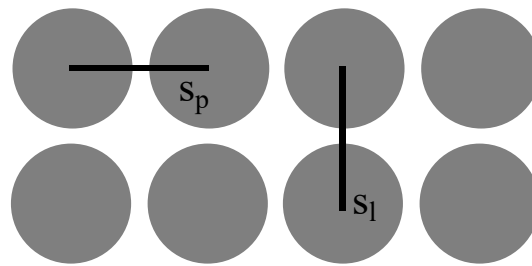


Fig. 5. Sketch of pulses with defined pulse spacing  $s_p$  and line spacing  $s_l$ .

The used scanner system is synchronized with the laser. This makes it possible to align the following lines directly under each other. However, it turns out that such an adjustment results in an additional low-frequency wave structure due to the difference of  $s_l$  and  $s_p$ . To avoid this, the waiting delays of the 8 polygon mirrors of the scanner were adjusted to create a kind of wobble in the starting point of the following lines (Fig. 6). These delays shift the starting point to a maximum of the half of  $s_p$ . If these settings are used a closed and regular wave structure can be produced. An image of such a structure can be seen in Fig. 7.

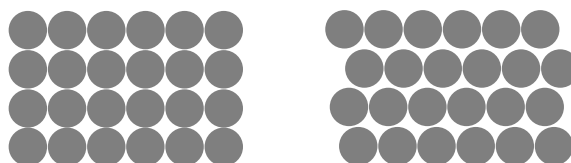


Fig. 6. Sketch of pulse arrays perfect orthogonal alignment (left) and aligned for areal LIPSS writing (right).

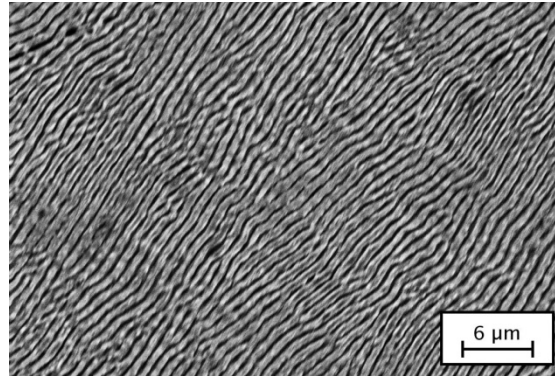


Fig. 7. SEM image of LIPSS with  $s_p = 28 \mu\text{m}$ ,  $s_l = 3 \mu\text{m}$  and desynchronized line alignment.

The scanning of predefined patterns can be achieved using bmp-files. The scanner performs a constant overwriting of the line and switches the laser on and off accordingly to the file data. If the sample is moved orthogonal to the scan direction (planar or cylindrical) a two-dimensional pattern can be produced. For this paper a large hexagonal pattern was used to test the precision and time dependence. To test also the industrial conditions a common Cr/Cu sleeve cylinder for printing or packaging technologies was used. Unfortunately due to the small line space of  $3 \mu\text{m}$  the bmp-file for a complete structuring of the sleeve is too large for standard encoders. This problem can be avoided by stitching several patterns together. The rotation speed of the sleeve is only determined by the line space. A line spacing of  $3 \mu\text{m}$  corresponds to a rotational speed of  $0.157 \text{ }^\circ/\text{s}$ . Using this a complete structuring of the sleeve can be achieved in only 38 min.

To test the lateral precision of the stitching process the original hexagonal pattern was separated into three files and processed on top of each other only changing the polarization of the laser beam. This results in an optical effect not only changing with the viewing angle but also with the rotational angle between sample and observer (Fig. 8). It was found that the precision of the process is equal to the precision of the axis ( $\sim 1 \mu\text{m}$ ).

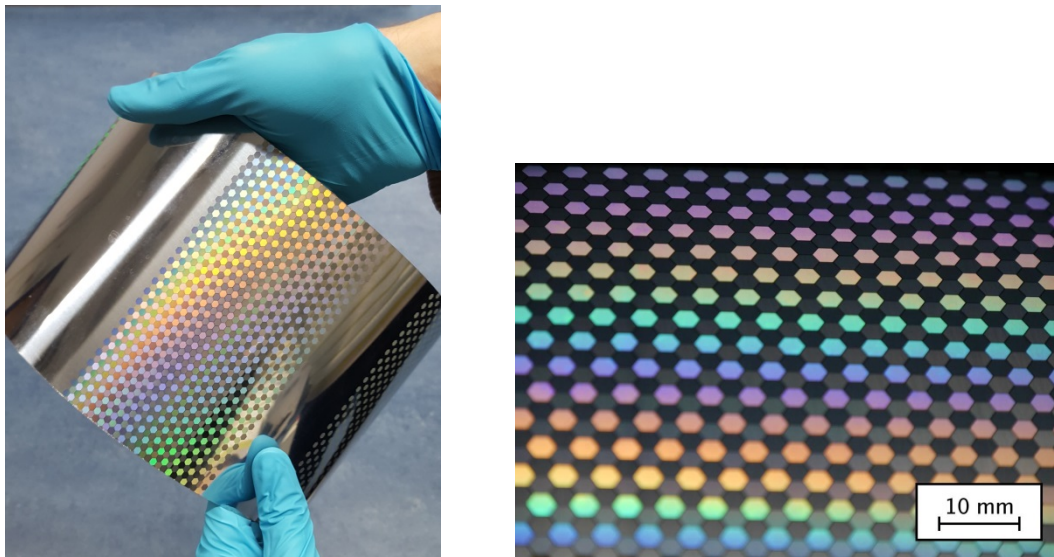


Fig. 8. Optical image of a hexagonal LIPSS pattern with different wave orientations, left: Cr-sleeve sample, right: close-up view with the different LIPSS orientation.

## 5. Conclusion

It was shown that laser-induced periodic surface structures (LIPSS) can be formed using a picosecond laser that provides a beam with a wavelength of  $1064 \text{ nm}$  and a pulse length of  $13 \text{ ps}$ . A parameter field was shown in which the structure is continuous and regular. Furthermore, problems and their solutions were discussed that emerge when using a high-speed polygon scanner system. It was shown that a structuring of large-area metal sleeves is possible in a reasonable commercial attractive time.

## References

- [1] Dusser, B., Sagan, Z., Soder, H., Faure, N., Colombier, J. P., Jourlin, M., Audouard, E., 2010. Controlled nanostructures formation by ultra fast laser pulses for color marking. *Optics Express*, 18, 2913–2924.
- [2] Groenendijk, M., Meijer, J., 2006. Microstructuring using femtosecond pulsed laser ablation. *Journal of Laser Applications*, 18, 227–235.
- [3] Long, J. Y., Fan, P. X., Zhong, M. L., Zhang, H. J., Xie, Y. D., Lin, C., 2014. Superhydrophobic and colorful copper surfaces fabricated by picosecond laser induced periodic nanostructures. *Applied Surface Science*, 311, 461–467.
- [4] Albu, C., Dinescu, A., Filipescu, M., Ulmeanu, M., Zamfirescu, M., 2013. Periodical structures induced by femtosecond laser on metals in air and liquid environments. *Applied Surface Science*, 278, 347–351.
- [5] Bonse, J., Krüger, J., Höhm, S., Rosenfeld, A., 2012. Femtosecond laser-induced periodic surface structures. *Journal of Laser Applications*, 24, 042006.
- [6] Emmony, D. C., Howson, R. P., Willis, L. J., 1973. Laser Mirror Damage in Germanium at 10.6  $\mu$ m. *Applied Physics Letters*, 23, 598–600.
- [7] Reif, J., Varlamova, O., Uhlig, S., Varlamov, S., Bestehorn, M., 2014. On the physics of self-organized nanostructure formation upon femtosecond laser ablation. *Applied Physics A – Materials Science & Processing*, 117, 179–184.
- [8] Tsibidis, G. D., Fotakis, C., Stratakis, E., 2015. From ripples to spikes: A hydrodynamical mechanism to interpret femtosecond laser-induced self-assembled structures. *Physical Review B*, 92, 041405.
- [9] Varlamova, O., Reif, J., Varlamov, S., Bestehorn, M., 2011. The laser polarization as control parameter in the formation of laser-induced periodic surface structures: Comparison of numerical and experimental results. *Applied Surface Science*, 257, 5465–5469.
- [10] Vorobyev, A. Y., Makin, V. S., Guo, C. L., 2007. Periodic ordering of random surface nanostructures induced by femtosecond laser pulses on metals. *Journal of Applied Physics*, 101, 034903.
- [11] Huynh, T. T. D., Semmar, N., 2014. Dependence of ablation threshold and LIPSS formation on copper thin films by accumulative UV picosecond laser shots. *Applied Physics A – Materials Science & Processing*, 116, 1429–1435.
- [12] Trtica, M. S., Gakovic, B. M., Radak, B. B., Batani, D., Desai, T., Bussoli, M., 2007. Periodic surface structures on crystalline silicon created by 532 nm picosecond Nd : YAG laser pulses. *Applied Surface Science*, 254, 1377–1381.
- [13] Sanz, M., Rebollar, E., Ganeev, R. A., Castillejo, M., 2013. Nanosecond laser-induced periodic surface structures on wide band-gap semiconductors. *Applied Surface Science*, 278, 325–329.
- [14] Rebollar, E., Castillejo, M., Ezquerro, T. A., 2015. Laser induced periodic surface structures on polymer films: From fundamentals to applications. *European Polymer Journal*, 73, 162–174.
- [15] Bäuerle, D., 2011, "*Laser processing and chemistry*". 4th ed., Springer, Berlin.